

© Copyright 2003 by the American Chemical Society

Unusual Reactions of the Model Carcinogen *N*-Acetoxy-*N*-acetyl-2-amino- α -carboline

Michael Novak* and Thach-Mien Nguyen

Department of Chemistry and Biochemistry, Miami University, Oxford, Ohio 45056

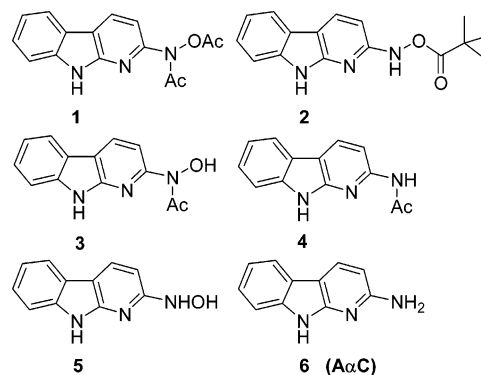
novakm@muohio.edu

Received April 18, 2003

The aqueous solution reactions of the title compound, **1**, were examined for comparison to those previously reported for another model carcinogen *N*-pivaloyloxy-2-amino- α -carboline, **2**. Both of these are models for the ultimate carcinogenic metabolites of 2-amino- α -carboline (A α C), a food-derived heterocyclic amine mutagen and carcinogen. The present study was undertaken to determine the effect of the *N*-acetyl group on the chemistry of such compounds. The *N*-acetyl group slows down N–O bond cleavage by a factor of (5.5×10^3) -fold. This allows other reactions not observed in **2**, or in other model carcinogens, to be observed. Among these are acyl-transfer reactions to the aqueous solvent, both uncatalyzed and catalyzed by N_3^- . In addition, the conjugate acid of **1**, **1H**⁺, is subject to a spontaneous decomposition not previously observed in other esters of heterocyclic hydroxylamines or hydroxamic acids. This reaction yields the hydroxylamine, **5**, and does so without the intermediacy of the hydroxamic acid, **3**, and with ¹⁸O exchange from the solvent into the hydroxylamine O. This unique reaction may be caused by an intramolecular proton donation by the pyridyl N–H to the amide carboxyl that catalyzes an intramolecular nucleophilic attack by the carboxyl O of **1H**⁺. A nitrenium ion pathway can still be detected for **1**, but, unlike **2** and related esters, this reaction is in competition with other processes throughout the pH range of the study.

Introduction

We have been involved in a long-term study of the aqueous solution chemistry of ester derivatives of heterocyclic *N*-arylhydroxylamines.^{1–3} These are the putative metabolites of heterocyclic amines generated during the cooking of protein-containing foods.^{4,5} Our studies



* Corresponding author.

(1) Novak, M.; Xu, L.; Wolf, R. A. *J. Am. Chem. Soc.* **1998**, *120*, 1643–1644.(2) Novak, M.; Kazerani, S. *J. Am. Chem. Soc.* **2000**, *122*, 3606–3616.(3) Novak, M.; Toth, K.; Rajagopal, S.; Brooks, M.; Hott, L. L.; Moslener, M. *J. Am. Chem. Soc.* **2002**, *124*, 7972–7981.(4) Eisenbrand, G.; Tang, W. *Toxicology* **1993**, *84*, 1–82. Hatch, F. T.; Knize, M. G.; Felton, J. S. *Environ. Mol. Mutagen.* **1991**, *17*, 4–19. Layton, D. W.; Bogen, K. T.; Knize, M. G.; Hatch, F. T.; Johnson, V. M.; Felton, J. S. *Carcinogenesis* **1995**, *16*, 39–52. Sugimura, T. *Mutat. Res.* **1985**, *150*, 33–41. Sugimura, T. *Environ. Health Perspect.* **1986**, *67*, 5–10. Ohgaki, H.; Takayama, S.; Sugimura, T. *Mutat. Res.* **1991**, *259*, 399–410. Felton, J. S.; Knize, M. G.; Shen, N. H.; Andersen, B. D.; Bjeldanes, L. F.; Hatch, F. T. *Environ. Health Perspect.* **1986**, *67*, 17–24.(5) Watanabe, M.; Ishidate, M.; Nohmi, T. *Mutat. Res.* **1990**, *234*, 337–348. Raza, H.; King, R. S.; Squires, R. B.; Guengerich, F. P.; Miller, D. W.; Freeman, J. P.; Lang, N. P.; Kadlubar, F. F. *Drug Metab. Dispos.* **1996**, *24*, 395–400. Pfau, W.; Brockstedt, U.; Schulze, C.; Neurath, G.; Marquardt, H. *Carcinogenesis* **1996**, *17*, 2727–2732. Pfau, W.; Schulze, C.; Shirai, T.; Hasegawa, R.; Brockstedt, U. *Chem. Res. Toxicol.* **1997**, *10*, 1192–1197. King, R. S.; Teitel, C. H.; Kadlubar, F. F. *Carcinogenesis* **2000**, *21*, 1347–1354. Frederiksen, H.; Frandsen, H. *Pharmacol. Toxicol.* **2002**, *90*, 127–134.

have shown that these esters generate heterocyclic *N*-arylnitrenium ions that react readily with N_3^- and with 2'-deoxyguanosine.^{1–3} For reasons of synthetic ease and stability of the model esters we have occasionally utilized esters of heterocyclic *N*-acetyl-*N*-arylhydroxylamines.³

Studies with carbocyclic analogues have shown that heterolytic N–O bond cleavage is slowed by a factor of up to 10^5 by replacement of NH with NAc in the esters, but the fundamental nature of the reaction is unaltered.^{6,7} The chemistry of the resulting nitrenium ion is only moderately altered by this replacement.^{6,7} Sites of reaction with nucleophiles are not altered, and the

TABLE 1. Kinetic and Thermodynamic Properties for 1 with Comparisons to 2

compd	k_A (s ⁻¹) ^a	k_B (s ⁻¹) ^a	pK_a	
			kinetic fit ^a	titration ^b
1 ^c	$(7.8 \pm 0.4) \times 10^{-4}$	$(9.8 \pm 0.4) \times 10^{-5}$	-0.08 ± 0.07	-0.04 ± 0.09
2 ^d				
compd	ΔH^\ddagger (kcal/mol) ^e	ΔS^\ddagger (cal/K·mol) ^e	$k_B(2)/k_B(1)$ ^f at 20 °C	$k_B K_a/k_A$ (M) from eq 2 ^g
1	16.4 ± 0.6	-25 ± 2	$(5.5 \pm 0.8) \times 10^3$	0.12 ± 0.02

^a From a weighted least-squares fit to eq 1. Values reported with their estimated standard deviations obtained from the fit. ^b From a fit of initial absorbance at 305 nm vs pH to a standard titration equation. ^c Conditions: 5 vol % of CH₃CN–H₂O, $\mu = 0.5$, $T = 40$ °C. ^d Conditions: 5 vol % of CH₃CN–H₂O, $\mu = 0.5$, $T = 20$ °C. Source: ref 2. ^e From a fit of $\ln(k_B/T)$ at pH 7.0 vs $1/T$ at 40, 50, and 60 °C. ^f From k_B for **1** extrapolated to 20 °C and k_B for **2** reported in ref 2. ^g Fit to eq 2 from product yield data for **5** (see Figure 3).

quantitative measure of reactivity and selectivity, k_{az}/k_s , the ratio of the second-order rate constant for reaction of the ion with N₃⁻ and the first-order rate constant for reaction with the aqueous solvent, is reduced by less than an order of magnitude by the *N*-acetyl group.^{6,7}

No comparative data have been available for heterocyclic *N*-arylnitrenium ions. For this reason we initiated a study of the chemistry of *N*-acetoxy-*N*-acetyl-2-amino- α -carboline, **1**, for comparison with our previously published study of the chemistry of *N*-pivaloyloxy-2-amino- α -carboline, **2**.² Both of these compounds are models for mutagenic and carcinogenic metabolites of the heterocyclic amine 2-amino- α -carboline, A α C.⁵ Our results show that the *N*-acetyl group can have a much more profound effect on the chemistry of these heterocyclic esters than anticipated from the results with carbocyclic esters.

Results and Discussion

Decomposition kinetics of **1** were monitored at 40 °C in 5 vol % of CH₃CN–H₂O. In the pH range (pH > 0.6) ionic strength, μ , was maintained at 0.5 with NaClO₄ and pH was maintained with HClO₄ (pH < 3.0) and with HCO₂H/HCO₂⁻, AcOH/AcO⁻, and H₂PO₄⁻/HPO₄²⁻ buffers. In more acidic solutions ($-2.0 \leq H_0 \leq 0.2$) no attempt was made to maintain constant μ , and acidity was maintained with HClO₄. H_0 values were obtained from the compilations of Paul and Long as revised by Yates and Wai.⁸

Kinetics monitored by UV methods generally did not fit well to a simple first-order rate equation, but could be fit to consecutive first-order rate equations containing two or three rate constants. Kinetics monitored by HPLC (Table S-1 of the Supporting Information) showed that **1** decomposed in a first-order fashion throughout the H_0 and pH range of the study, but that two initial reaction products, the hydroxamic acid, **3**, and the amide, **4**, underwent further hydrolysis into the corresponding hydroxylamine, **5**, and the amine, **6**, respectively (Tables S-2 and S-3 of the Supporting Information).

Table S-1 shows that the rate constant k_1 for the decomposition of **1** obtained from HPLC measurements is in good agreement with a rate constant, also assigned as k_1 , observed by UV methods. The data show that k_1 is buffer independent, but does exhibit pH dependence. A

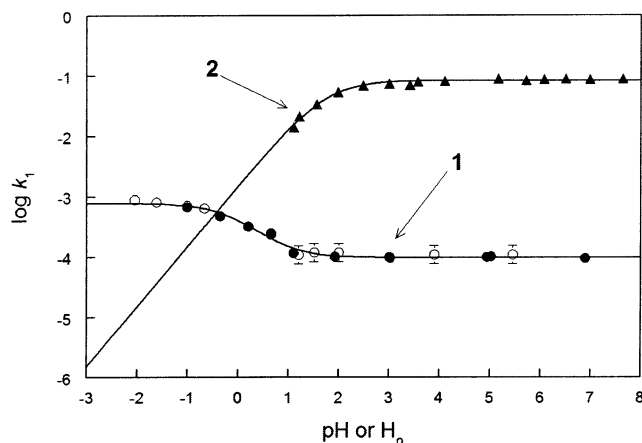


FIGURE 1. Log k_1 vs pH for **1** and **2**. Rate constants for **1** come from HPLC (●) and UV (○) measurements at 40 °C. Data for **2** (▲) are from UV measurements at 20 °C reported in ref 2. Data were fit to eq 1 for **1** and to the second term of eq 1 for **2**.

plot of log k_1 for **1** vs H_0 or pH (Figure 1) is qualitatively and quantitatively quite different from the plot of log k_1 for **2** obtained at 20 °C from the previously reported study.² The data for k_1 of **1** were fit well by eq 1,

$$k_1 = (10^{(-x)}k_A + K_a k_B)/(K_a + 10^{(-x)}) \quad (1)$$

where $x = H_0$ or pH. Equation 1 indicates that both **1** and **1H**⁺, its conjugate acid, are subject to spontaneous uncatalyzed decomposition. The data for **2** were previously fit to the second term of eq 1 ($K_a k_B/(K_a + 10^{(-x)})$), a term consistent with rate-limiting N–O bond cleavage.² Kinetic parameters obtained from the fits are reported in Table 1. The kinetically obtained pK_a for **1H**⁺ is in excellent agreement with the pK_a obtained by fitting initial absorbance of **1** at 305 nm vs pH (or H_0) to a standard titration equation (Table 1). The pK_a of **1H**⁺ is about 1.8 units more negative than that for **2H**⁺ (Table 1), while k_B for **2** is (5.5×10^3) -fold larger than k_B for **1** extrapolated to 20 °C from data taken at 40, 50, and 60 °C in pH 7.0 phosphate buffers. The effect of the *N*-acetyl group on pK_a is consistent with the electron-withdrawing effect of the acetyl group relative to H. The rate effect on k_B is also consistent with expectations for a rate-limiting transition state that involves generation of a positive charge on the exocyclic N.^{6,7} The sign and magnitude of ΔS^\ddagger (Table 1) for k_B suggest a highly ordered transition state that is consistent with restricted rotation about the C–N bond of an incipient nitrenium

(6) Novak, M.; Kahley, M. J.; Eiger, E.; Helmick, J. S.; Peters, H. E. *J. Am. Chem. Soc.* **1993**, *115*, 9453–9460.

(7) Novak, M.; Rajagopal, S. *Adv. Phys. Org. Chem.* **2001**, *36*, 167–254.

(8) Paul, M. A.; Long, F. A. *Chem. Rev.* **1957**, *57*, 1–45. Yates, K.; Wai, H. *J. Am. Chem. Soc.* **1964**, *86*, 5408–5413.

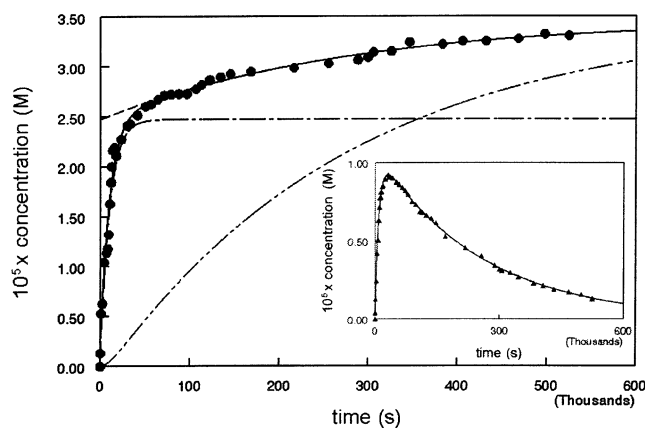
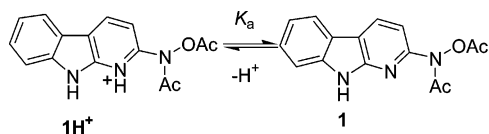


FIGURE 2. Plot of the time course for appearance of **5** (●) and **3** (▲) during the decomposition of **1** at pH 1.10: (solid lines) the fits of the data to a consecutive first-order rate equation containing two rate constants; (— —) the component of the time course of **5** attributable to hydrolysis of **3**; (— · —) the component of the time course of **5** attributable to the fast process not involving **3**; (· · ·) the predicted time course for the appearance of **5** if all of it were produced by hydrolysis of **3** (see ref 10).

ion. The *N*-sulfonatoxyacetanilides, which also generate *N*-acetylnitrenium ions, exhibit ΔS^\ddagger of the same sign and similar magnitude in the same solvent system.⁹

The k_A term shows that **1H⁺** is (8.0 ± 0.5) -fold more reactive than **1** toward spontaneous decomposition in our solvent system. This behavior has not been observed



previously. The conjugate acids of the Glu-P-1 and Glu-P-2 derivatives **7a** and **7b** are subject to acid-catalyzed decomposition, but no spontaneous decomposition of the protonated species was reported.³ If k_A is included in a fit of the data previously reported for **7a**, this term is not statistically significant at the 95% confidence level. Such a term is statistically significant at the 95% confidence level in a fit performed on the previously reported data for **7b**, but it is kinetically insignificant. Its magnitude is 100-fold smaller than that of the k_B term for **7b**, and it is always dominated by the acid-catalyzed term under conditions in which **7bH⁺** is present in significant concentrations. Spontaneous uncatalyzed decomposition of **7aH⁺** and **7bH⁺** is clearly not important if it occurs at all.

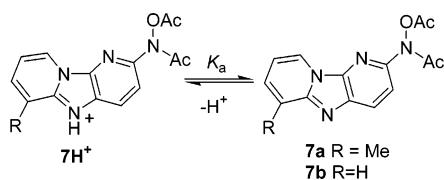


Figure 2 shows the time course for generation of the hydroxamic acid **3** and the hydroxylamine **5** at pH 1.10. The majority of **5** (70%) is formed rapidly from **1** without an apparent intermediate and with a rate constant that is consistent (Tables S-1 and S-2) with the magnitude of

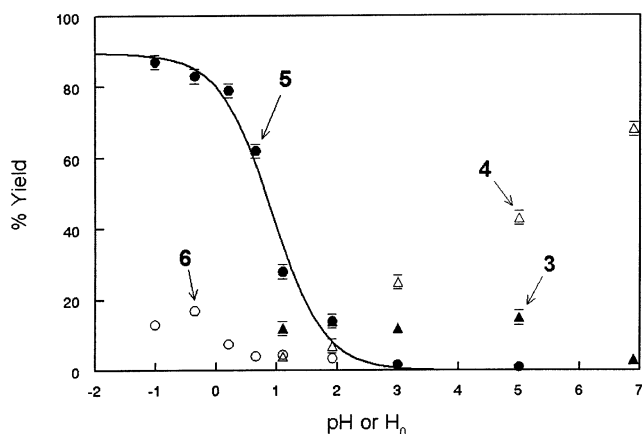


FIGURE 3. Plot of product yields vs pH for **3**, **4**, **5**, and **6**. Symbols are identified in the figure. The line is a least-squares fit of the data for **5** to eq 2.

k_1 measured for the disappearance of **1**. Only 30% of **5** is generated in a slower process consistent with the magnitude of k_2 , the rate constant for hydrolysis of **3** (Tables S-2 and S-3). Figure 2 shows that the time course for the appearance of **5** would be very different if all of it were generated from hydrolysis of **3**.¹⁰ A similar observation was made at pH 1.92 except that in this case 51% of **5** is formed without the intermediacy of **3**. At higher pH, **3** is stable enough (Table S-3) that no significant decomposition of it occurs (<5%) during the time it takes for the decomposition of **1** to reach 10 half-lives. The small amount of **5** observed in this pH range is formed with a rate constant consistent with k_1 , not by slow decomposition of **3**. At pH <1.0, **5** is the major reaction product (Figure 3). In this pH range it is generated via a first-order process with a rate constant equivalent to k_1 (Table S-2). Although **3** decomposes fairly rapidly in this pH range (Table S-3), it would have been detected by HPLC if generated in significant quantities during the decomposition of **1**. It appears that in this pH range all of the observed **5** is generated directly from **1** without the intermediacy of **3**. Similar conclusions can be made concerning the amine, **6**. Significant amounts of **6** are detected only at pH ≤ 2.0 , and it is always a minor product compared to **5**. At $1.0 \leq \text{pH} \leq 2.0$ some of **6** is generated from hydrolysis of **4** governed by the rate constant k_3 , but in more acidic solutions all of **6** appears to be generated directly from **1**.

Figure 3 shows the pH dependence of the product yields for the four major reaction products **3**, **4**, **5**, and **6**. In this figure yields for **5** and **6** are the yields of those products obtained directly from **1** without the intermediacy of **3** and **4**. The yields of **3** and **4** are extrapolated from the kinetic data in the pH range in which they exhibit significant decomposition, so **5** and **6** generated from hydrolysis of **3** and **4** are included as part of the yields of **3** and **4**. Recovery is significantly below 50% at $1 < \text{pH} < 5$. The yield of one product, **5**, varies with pH in a manner that is directly related to the kinetic results. If it is assumed that **5** is generated only by the k_A process,

(9) Novak, M.; Pelecanou, M.; Roy, A. K.; Andronico, A. F.; Plourde, F. M.; Olefirowicz, T. M.; Curtin, T. J. *J. Am. Chem. Soc.* **1984**, *106*, 5623–5631.

(10) Novak, M.; Roy, A. K. *J. Org. Chem.* **1985**, *50*, 571–580.

TABLE 2. ^{18}O Analysis of **3** and **5** Generated from **1** at pH 1.10 in 47.6 mol % ^{18}O -Enriched H_2O and in Ordinary H_2O

compd	expt no.	experiment ^a	$100 \times (M + 3) / [(M + 1) + (M + 3)]^b$
3	1	1 in ^{18}O -enriched H_2O	5.76 ± 0.26
3	2	1 in ordinary H_2O	0.88 ± 0.26
3	3	3 in ^{18}O -enriched H_2O	2.63 ± 0.40
3	4	3 in ordinary H_2O	0.66 ± 0.08
5	1	1 in ^{18}O -enriched H_2O	38.71 ± 0.08
5	2	1 in ordinary H_2O	1.07 ± 0.23
5	5	5 in ^{18}O -enriched H_2O	1.16 ± 0.05
5	6	5 in ordinary H_2O	1.33 ± 0.37

^a All compounds were incubated in the pH 1.1 solvent at 40 °C for 6.5 h before neutralization with 0.02 M $\text{H}_2\text{O}_4^-/\text{HPO}_4^{2-}$ pH 6.8 buffer, extraction with CH_2Cl_2 , solvent evaporation. Residue was taken up in MeOH immediately prior to analysis. ^b Calculated from integrated peak intensities for the $(M + 1)^+$ and $(M + 3)^+$ ions obtained by LC/MS analysis, using an APCI source.

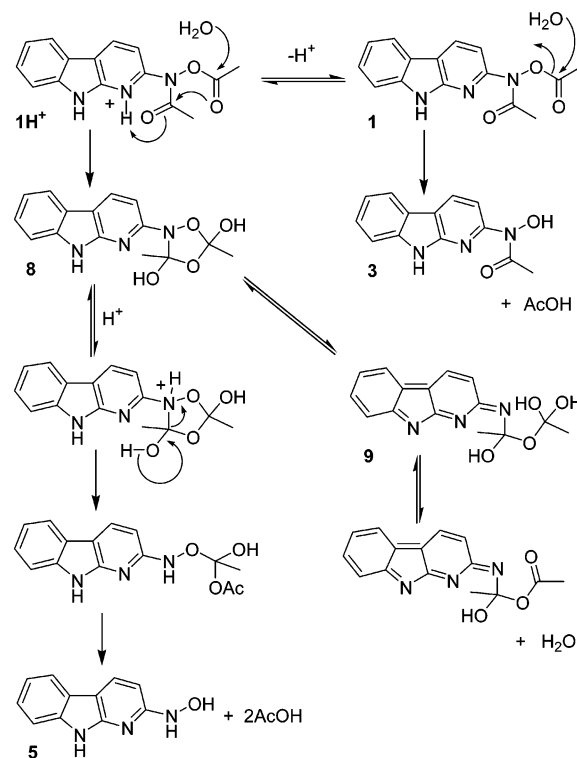
its yield should vary with pH according to eq 2

$$\% \text{ of } \mathbf{5} = f_5 10^{(-x)} / (10^{(-x)} + K_a k_B / k_A) \quad (2)$$

where $x = H_0$ or pH. A least-squares fit of the percent yield data for **5** as a function of pH provides $f_5 = (90 \pm 3)\%$ and $K_a k_B / k_A = (0.12 \pm 0.02)$ M (Table 1). The value of $K_a k_B / k_A$ derived from the kinetic fit is (0.15 ± 0.03) M. It appears that **5** directly formed from **1** is generated exclusively by the k_A process.

The chemical processes leading to **3** and **5** during the decomposition of **1** were probed by experiments performed in 47.6 mol % of ^{18}O -enriched H_2O at pH 1.10 and 40 °C. The ^{18}O content of **3** and **5** was calculated from the peak intensities for the $(M + 3)^+$ and $(M + 1)^+$ ions produced from an APCI source of an LC/MS. All experiments were run for 6.5 h, the time at which the maximum yield of **3** is obtained at this pH. At this reaction time 96% of **5** is generated by the faster process (k_1) that does not involve **3** according to the kinetic data. Experimental results are summarized in Table 2. Analysis shows an excess incorporation of $(4.88 \pm 0.37)\%$ of ^{18}O into **3** formed from **1** in the ^{18}O -enriched H_2O (expt no. 1–expt no. 2 in Table 2). Control experiments show that $(1.97 \pm 0.41)\%$ of this is accounted for by ^{18}O exchange into **3** during the experiment (expt no. 3 – expt no. 4). The difference, $(2.91 \pm 0.55)\%$, represents the maximum excess ^{18}O incorporation into **3** during the decomposition of **1**. This is a maximum because some ^{18}O incorporation into the amide carboxyl O of **1** may occur during the experiment. This would be transferred to the carboxyl O of **3** and would contribute to the $(M + 3)^+$ peak intensity. The small amount of **1** present at the 6.5 h reaction time and the low intensity of its $(M + 1)^+$ peak precluded direct measurement of ^{18}O incorporation into **1**. In any case, this result could not distinguish between ^{18}O incorporation into the amide carboxyl O or the ester carboxyl O. The results show that a minimum of 94% of **3** is generated by a process that involves no ^{18}O exchange.

In contrast, considerable ^{18}O exchange occurs into **5**. An excess ^{18}O incorporation of $(37.64 \pm 0.24)\%$ is observed (expt no. 1 – expt no. 2). None of this can be attributed to ^{18}O exchange into **5** after it is generated (expt no. 5 – expt no. 6). The results show that 79% of the theoretical maximum exchange occurs during formation of **5**.

SCHEME 1

A mechanism for the formation of **3** and **5** that is consistent with the experimental data is shown in Scheme 1. The hydroxamic acid, **3**, appears to be generated from the neutral species **1** because it is not detected at pH < 1. The ^{18}O exchange data are consistent with a simple acyl-transfer reaction with the hydroxamic acid serving as the leaving group. This acyl-transfer reaction has not previously been observed for **7a**, **7b**, or related heterocyclic esters.³ These esters are more reactive toward N–O bond cleavage than **1**, so a slow acyl-transfer reaction would not be detected for these compounds. Even in the case of **1**, **3** is a minor product with a yield that does not exceed 15%. The data show that **5** not produced by hydrolysis of **3** is generated entirely from **1H**⁺. The pyridyl proton may catalyze an intramolecular nucleophilic attack of the ester carboxyl O on the amide that is initiated by attack of H_2O on the ester. This would generate the cyclic intermediate **8**. Reversible N–O bond cleavage in this species to generate **9** could account for the ^{18}O exchange with solvent. The exchange in excess of that predicted from reversible generation of **9** (23.8% from 47.6 mol % of ^{18}O -enriched H_2O) can be accounted for if **9** reversibly lost H_2O to the solvent under the acidic reaction conditions. Protonation of the N of the 1,4,2-dioxazolidine ring of **8** would lead to decomposition of **8** generating the hydroxylamine, **5**. Other mechanisms could be written for this process, but they all must be consistent with spontaneous decomposition of **1H**⁺, ^{18}O exchange into the hydroxylamine product, and the lack of involvement of the hydroxamic acid as an intermediate. This spontaneous reaction of the protonated ester has not previously been observed with **7a** or **7b**.³ The reason for this could be the unique pyridyl protonation site of **1**. Both **7a** and **7b** are predominately protonated at a different site (see **7aH**⁺ and **7bH**⁺) that would not allow for the cyclic transition state shown in Scheme 1.³

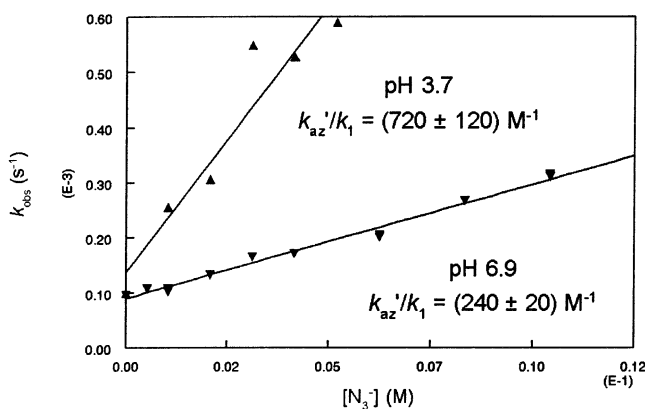


FIGURE 4. Plots of k_{obs} for the disappearance of **1** vs $[\text{N}_3^-]$ at pH 3.7 (\blacktriangle) and pH 6.9 (\blacktriangledown). The lines are a linear least-squares fit of the data. The values of k_{az}'/k_1 are the slope/intercept of the least-squares fit.

TABLE 3. Azide Trapping Results

pH	$10^{-2}k_{\text{az}}'/k_1$ (M^{-1}) ^a		$10^{-2}k_{\text{az}}/k_{\text{c}}$ (M^{-1}) ^a	
	from kinetics	from 3	from 4	from 10
6.9	2.4 ± 0.2	3.3 ± 0.7	6.0 ± 0.8	2.9 ± 0.7
3.7	7.2 ± 1.2	5.7 ± 0.8		12 ± 3

^a Ratios reported with their estimated standard deviations from fits to the equations shown in the text.

Figure 4 shows that k_{obs} varies linearly with $[\text{N}_3^-]$ in 0.02 M $\text{H}_2\text{PO}_4^-/\text{HPO}_4^{2-}$ buffers (pH 6.9) and in 0.02 M AcOH/AcO^- buffers (pH 3.7). Previously, rate constants for the decomposition of other esters of heterocyclic hydroxamic acids, including **7a** and **7b**, have been shown to be insensitive to $[\text{N}_3^-]$.³ The greater sensitivity to $[\text{N}_3^-]$ at lower pH indicates that **1H**⁺ reacts more readily with N_3^- than does **1**, but the N_3^- -dependence is significant under both pH conditions. Second-order rate constants for reaction of N_3^- with **1** and **1H**⁺, k_{azB} and k_{azA} , are $2.4 \times 10^{-2} \text{ M}^{-1} \text{ s}^{-1}$ and $2.9 \times 10^2 \text{ M}^{-1} \text{ s}^{-1}$, respectively, assuming the $\text{p}K_{\text{a}}$ for **1H**⁺ shown in Table 3 and k_1 at both pH values of ca. $1 \times 10^{-4} \text{ s}^{-1}$.

The nature of this second-order process is revealed by the product data in Figure 5. The hydroxamic acid, **3**, is produced at the expense of the amide, **4**, as $[\text{N}_3^-]$ increases. A fit of **[3]** at pH 6.9 to eq 3, where **[3]₀**, **[3]_{max}**, and k_{az}'/k_1 are adjustable parameters, is shown in Figure 5. The parameter **[3]₀** is required because there is a small,

$$[\mathbf{3}] = ([\mathbf{3}]_0 + (k_{\text{az}}'/k_1)[\text{N}_3^-][\mathbf{3}]_{\text{max}})/(1 + (k_{\text{az}}'/k_1)[\text{N}_3^-]) \quad (3)$$

but measurable, yield of **3** in the absence of N_3^- . The value of k_{az}'/k_1 obtained from the fit at pH 6.9 of $(330 \pm 70) \text{ M}^{-1}$ is in reasonable agreement with the rate constant ratio calculated from the kinetic data (Table 3). At pH 3.7 similar agreement is obtained. It is clear that N_3^- reacts selectively with the acetoxy group of **1** or **1H**⁺ to catalyze a C–O bond cleavage reaction that generates **3**. Presumably this reaction has not been observed with other esters of heterocyclic hydroxamic acids because they exhibit much more rapid N–O bond cleavage than does **1** (30- to 1300-fold larger rate constants under the same conditions).³ At the low N_3^- concentrations used in these studies ($\leq 10 \text{ mM}$), the rate accelerations caused

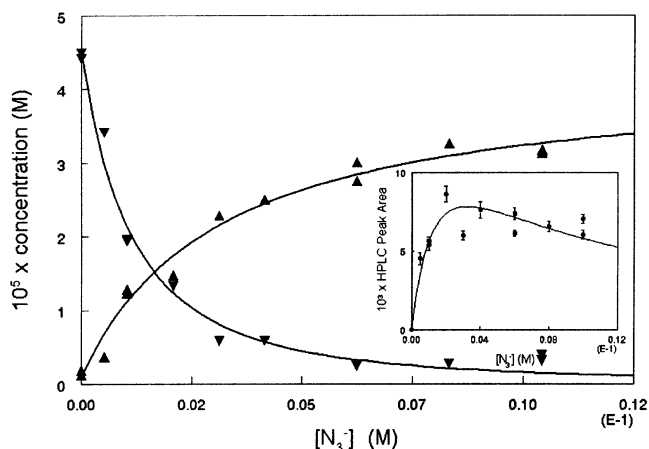


FIGURE 5. Plot of the yields of **3** (\blacktriangle), **4** (\blacktriangledown), and **10** (insert, \bullet) as a function of $[\text{N}_3^-]$ at pH 6.9. Data were fit to eqs 3 (for **3**), 4 (for **4**), and 5 (for **10**) as described in the text.

by this reaction would be $\leq 5\%$ if the sensitivity of these esters to the second-order reaction with N_3^- is about the same as that for **1**.

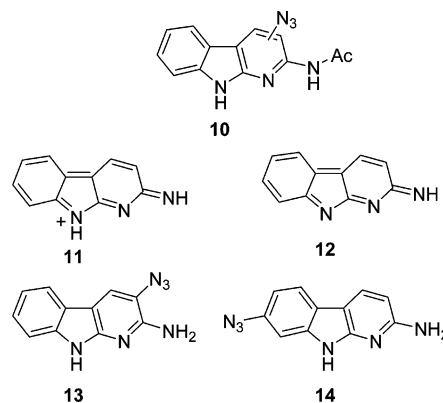
The amide, **4**, disappears with increasing $[\text{N}_3^-]$ to a greater extent than can be accounted for by the k_{az}'/k_1 partitioning. A new product also appears in the presence of N_3^- . This material was not isolated because of its low yield, but mass spectrometric data taken by LC/MS are consistent with an N_3^- -adduct represented by structure **10**. The observed yields of both **4** and **10** as a function of $[\text{N}_3^-]$ were fit to eqs 4 and 5, respectively.

$$[\mathbf{4}] = [\mathbf{4}]_{\text{max}}(1/(1 + (k_{\text{az}}'/k_1)[\text{N}_3^-]))/(1 + (k_{\text{az}}/k_{\text{c}})[\text{N}_3^-]) \quad (4)$$

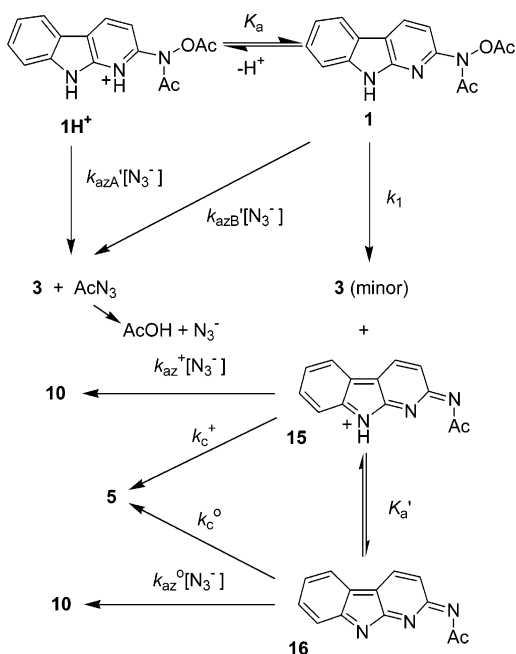
$$[\mathbf{10}] = [\mathbf{10}]_{\text{max}}(1/(1 + (k_{\text{az}}'/k_1)[\text{N}_3^-]))((k_{\text{az}}/k_{\text{c}})[\text{N}_3^-]/(1 + (k_{\text{az}}/k_{\text{c}})[\text{N}_3^-])) \quad (5)$$

In each case the value of k_{az}'/k_1 employed was that obtained from the fit of the yield of **3** to eq 3. The other two parameters ($[\mathbf{4}]_{\text{max}}$ or $[\mathbf{10}]_{\text{max}}$ and $k_{\text{az}}/k_{\text{c}}$) were adjustable least-squares parameters. The fits at pH 6.9 are shown in Figure 5. Equations 4 and 5 are consistent with a second N_3^- -dependent partitioning process that occurs after the original k_{az}'/k_1 partitioning.

In the previous study involving **2**, pH-dependent trapping of an intermediate nitrenium ion, **11**, and its quinonoid-like conjugate base, **12**, was invoked to explain the effects of N_3^- and Br^- on product distributions and



SCHEME 2



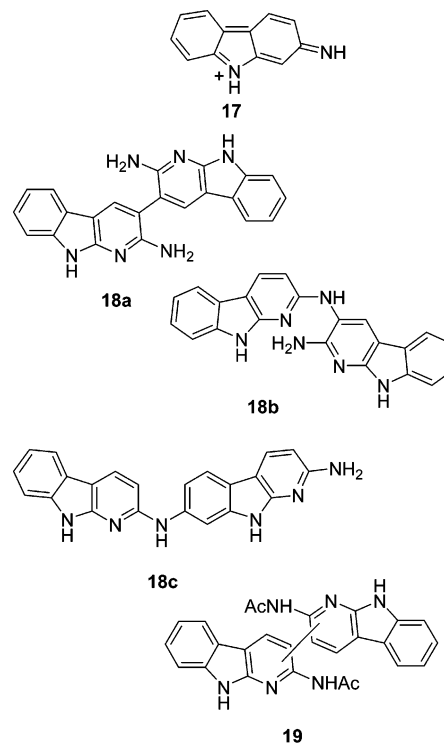
identities.² The major reaction product of **2** in the absence of N_3^- was the reduction product **6** (ca. 50% at neutral pH, and 20% at pH <4.0).² The analogous product **4** is the major observed product of **1** from pH 3.0 to 7.0, and, similar to **6**, its yield decreases as pH decreases in that range. The hydroxylamine ester **2** was not subject to an N_3^- -dependent second-order rate acceleration, but the yield of **4** did decrease in the presence of N_3^- , and the two N_3^- -adducts **13** and **14** were formed in its place.² The N_3^- trapping and results of trapping experiments performed with H^- donors suggested that **6** was produced by reduction of singlet **11** and, predominately, **12**, not a triplet or radical species.² The species responsible for the reduction was not identified, but it could be other reaction products generated by **2**.

The effects of N_3^- on the reactions of **1** can be explained by the mechanism of Scheme 2. The nitrenium ion component of this mechanism is identical with that previously proposed for **2**.² Since N_3^- clearly increases the rate of decomposition of **1** and **1H⁺** to generate the hydroxamic acid, **3**, nucleophilic catalysis of acyl transfer by N_3^- on both **1** and **1H⁺** is included. This process is in competition with the k_1 process for **1** that leads predominately, but not exclusively, to N–O bond cleavage. N_3^- also affects distribution of products derived from the nitrenium ion, **15**, and its conjugate base, **16**. The conjugate acid–base pair is invoked because there is evidence, based on data taken at two pH values (Table 3), that the extent of N_3^- -trapping at this stage is pH-dependent. It is not possible to determine the two limiting trapping ratios, $k_{\text{az}}^+/k_{\text{c}}^+$ and $k_{\text{az}}^{\circ}/k_{\text{c}}^{\circ}$, with only two data points without knowledge of $-\log(K_{\text{a}}'k_{\text{c}}^{\circ}/k_{\text{c}}^+)$, $\text{p}K_{\text{a}}'^{\text{app}}$, obtained from a fit of $k_{\text{az}}/k_{\text{c}}$ to $[\text{H}^+]$ (eq 6).² For **11**, $\text{p}K_{\text{a}}'^{\text{app}}$

$$k_{\text{az}}/k_{\text{c}} = (k_{\text{az}}^+[\text{H}^+]/k_{\text{c}}^+ + k_{\text{az}}^{\circ}K_{\text{a}}'^{\text{app}}/k_{\text{c}}^{\circ})/([\text{H}^+] + K_{\text{a}}'^{\text{app}}) \quad (6)$$

is 4.9, while it is 7.7 for the related 2-carbazolylnitrenium ion, **17**, that also undergoes deprotonation to a neutral

quinonoid-like conjugate base.^{2,11} The *N*-acetyl group of **15** should lower $\text{p}K_{\text{a}}'^{\text{app}}$ below that of **11**. Therefore, the observed value of $k_{\text{az}}/k_{\text{c}}$ at pH 6.9 should be a good approximation to $k_{\text{az}}^{\circ}/k_{\text{c}}^{\circ}$. The values of $k_{\text{az}}/k_{\text{c}}$ obtained from **4** and **10** at pH 6.9 (Table 3) are in modest agreement (within 2 standard deviations). The average value of 450 M^{-1} is ca. 2.7-fold smaller than the value of $1.2 \times 10^3 \text{ M}^{-1}$ reported for $k_{\text{az}}^{\circ}/k_{\text{c}}^{\circ}$ for **12**.²



The *N*-acetyl group lowers the $\text{p}K_{\text{a}}$ of **1H⁺** by 1.8 units compared to that for **2H⁺**. If this is taken as an estimate for the effect of the *N*-acetyl group on $\text{p}K_{\text{a}}'^{\text{app}}$ for **11**, the estimated $\text{p}K_{\text{a}}'^{\text{app}}$ for **15** is ca. 3.1. If that value of $\text{p}K_{\text{a}}'^{\text{app}}$ is substituted into eq 6 with the observed value of $k_{\text{az}}/k_{\text{c}}$ at pH 3.7 (Table 3), and $k_{\text{az}}^{\circ}/k_{\text{c}}^{\circ}$ estimated above, $k_{\text{az}}^+/k_{\text{c}}^+$ is estimated to be $4.2 \times 10^3 \text{ M}^{-1}$. The error limit on this number is estimated to be $\pm 50\%$, but it is only 8-fold smaller than $k_{\text{az}}^+/k_{\text{c}}^+$ for **11**.² This result suggests that the effect of the *N*-acetyl group on the selectivity of **15** is similar to that previously observed for carbocyclic *N*-acetyl-*N*-arylnitrenium ions.^{6,7}

Other products attributed to the nitrenium ion pathway for **2** included the dimers **18a–c** that appeared to be generated by attack of the amine, **6**, on the nitrenium ion **11** or its conjugate base **12**.² These dimers are unusual products that are not observed in other studies involving heterocyclic or carbocyclic *N*-arylnitrenium ions because significant concentrations of the amine or amide reduction products are usually not present during these reactions.^{1,3,6,7} The dimers appear to be formed because of the propensity for reduction of **11** and **12**, and their relatively long lifetime, so that they can be nucleophilically trapped by their own reduction product.² It has been shown in other studies that aromatic amines such as

(11) McClelland, R. A.; Licence, V. E. *Arkivoc* **2001**, 12, 72–81 (<http://www.arkat-usa.org/ark/journal/Volume2/Part3/Tee/OT-286C/OT-286C.pdf>).

aniline and *N,N*-dimethylaniline are excellent traps for *N*-arylnitrenium ions.¹² There is another recent example of a long-lived cation (α -(*N,N*-dimethylthiocarbamoyl)-4-methoxybenzyl cation) that reacts with its own elimination product to form a dimer because of the long lifetime of the cation.¹³ Increasing solvent nucleophilicity suppresses the formation of this dimer.¹³ In the present study a product with HPLC retention time and mass spectrum consistent with the dimeric structure **19** was detected by LC/MS in reaction mixtures of **1** in the pH range 3.0 to 5.0. This provides further evidence that the nitrenium ion path occurs for **1** despite the many differences in the chemistry of **1** and **2**.

In conclusion, the addition of the *N*-acetyl group to form **1** results in significant suppression of the rate of the N–O bond cleavage process in H₂O so that competing reactions that are not observed in other model esters for carcinogens derived from heterocyclic amines can be detected. Included among these are a slow uncatalyzed acyl-transfer to the solvent, a more rapid acyl-transfer catalyzed by N₃[−], and an apparently unique spontaneous decomposition of the conjugate acid of **1**, **1H**⁺, that may be facilitated by an intramolecular proton transfer. Although the nitrenium ion path is kinetically suppressed by the electron-withdrawing *N*-acetyl group, it still appears to be the dominant process at neutral pH in the absence of strong nucleophiles such as N₃[−]. The properties of the nitrenium ion **15** and its conjugate base **16** appear to be similar to those of the deacetylated analogues **11** and **12**.

Experimental Section

General Procedures. The synthesis and characterization of **1**, **3**, and **4** are described in the Supporting Information. All other isolated compounds are described in the literature.¹⁴ All salts used for preparation of buffers were reagent grade. The purification of CH₃CN and DMF was carried out according to the method described elsewhere.¹⁵ Water used in all the experiments and kinetic studies was distilled, deionized, and distilled again. All other reagents and solvents were reagent grade and distilled. General procedures for preparing solutions, measuring rate constants by UV and HPLC methods, and analyzing products by HPLC methods have been described elsewhere.^{2,6,9,10}

Kinetics and Product Studies. The kinetic study for **1** was performed in 5 vol % of CH₃CN–H₂O solutions, $\mu = 0.5$ (NaClO₄), $T = 40$ °C, unless otherwise stated. To maintain pH, NaH₂PO₄/Na₂HPO₄ (pH 5.5–7.5), AcOH/AcONa (pH 4.0–5.0), and HCOOH/HCOONa (pH 3.0–3.5) buffers were employed. HClO₄ solutions were used at pH <3.0, and in the *H*₀ region where ionic strength was not maintained.

To carry out the reaction, 15 μ L of a 0.001 or 0.01 M stock solution of **1** in DMF was injected into 3 mL of the appropriate solution to obtain initial concentrations of **1** of 5×10^{-6} or 5×10^{-5} M. The solution was incubated for at least 15 min prior to initiation of the reaction at 40 °C in either a thermostated cell (when using the UV spectrophotometer) or a water bath (when monitoring the reaction by HPLC). For the HPLC method, peak area vs time data for the starting material and

products were examined. For the UV method, absorbance at 305 or 275 nm was plotted against time. The UV and HPLC data were fit by nonlinear least-squares methods to the standard first-order rate equation or to consecutive first-order rate equations. The HPLC conditions were the following: UV detection at 320 nm, 55/45 MeOH/H₂O eluent buffered with 0.025 M 1:1 HOAc:KOAc, C-18 reverse-phase column, 1 mL/min flow rate.

Similar procedures were followed for kinetic measurements involving **3** and **4**. To carry out the reaction, 15 μ L of a 0.002 M stock solution of **3** or **4** in DMF was injected into 3 mL of the appropriate solution incubated in a 40 °C water bath to obtain an initial concentration of 1×10^{-5} M. HPLC data were fit by nonlinear least-squares methods to the standard first-order rate equation. Rate constants for very slow reactions ($k_{\text{obs}} < 10^{-6} \text{ s}^{-1}$) were determined by initial rates methods from the slope of a plot of reactant HPLC peak area vs time for the first 5% of the reaction.

The products of the decomposition of **1** were monitored by HPLC and LC/MS under conditions identical with those used for the kinetic studies. The major products **3**, **4**, **5**, and **6** were identified by co-injection with authentic compounds, and by comparison of mass spectra obtained by LC/MS with those of the authentic compounds. When **1** decomposed at pH 3.0 and 5.0, a small amount of a dimer (**19**) was observed by HPLC with 75/25 MeOH/H₂O as eluent. LC-MS (APCI, positive ion mode) C₂₆H₂₁N₆O₂ (M + H)⁺ calcd *m/e* 449.15, found 449.20. At pH 6.9, during the decomposition of **1** in the presence of N₃[−], the azide adduct **10** was observed. LC-MS (ESI, positive ion mode) C₁₃H₁₁N₄O (M – N₂ + H)⁺ calcd *m/e* 239.28, found 239.70.

¹⁸O Exchange into **3 and **5**.** The ¹⁸O-enriched solution (1 mL) was made with 0.10 mL of 1 M HClO₄, 0.05 mL of CH₃CN, 0.375 mL of distilled H₂O, and 0.475 mL of 95 atom % of ¹⁸O-enriched H₂¹⁸O. An ionic strength of 0.5 was maintained with 0.0562 g of NaClO₄. Reactions were performed as described above for the kinetics experiments. After 6.5 h, the reaction solution was neutralized to pH 5.0 by addition of 1.5 mL of 0.02 M phosphate buffer (pH 6.80) and then extracted with 3×1 mL of CH₂Cl₂. The CH₂Cl₂ was evaporated, without predrying. The solid was immediately redissolved in MeOH and subjected to LC/MS to analyze the ¹⁸O content of **3** and **5**. Controls in which **3** and **5** were incubated in the ¹⁸O-enriched solution for 6.5 h were performed, as were controls for **1**, **3**, and **5** in ordinary unenriched pH 1.1 solution. In each of these experiments, analyses for the ¹⁸O content of **3** and **5** was performed by obtaining the integrated peak intensities for the (M + 1)⁺ and (M + 3)⁺ ions. For **3**, LC/MS (APCI, positive ion mode) C₁₃H₁₂N₃¹⁶O₂ (M + H)⁺ calcd *m/e* 242.26, found 242.10, and C₁₃H₁₂N₃¹⁸O¹⁶O (M + H)⁺ calcd *m/e* 244.27, found 244.00. For **5**, LC/MS (APCI positive ion mode) C₁₁H₁₀N₃¹⁶O (M + H)⁺ calcd *m/e* 200.08, found 200.10, and C₁₁H₁₀N₃¹⁸O (M + H)⁺ calcd *m/e* 202.09, found 202.10.

Acknowledgment. This work was supported by a grant from the American Cancer Society (RPG-96-078-03-CNE). NMR spectra were obtained on equipment made available through an NSF grant (CHE-9012532) and upgraded through an Ohio Board of Regents Investment Fund grant. LC/MS were obtained on equipment made available through an Ohio Board of Regents Investment Fund grant. High-resolution mass spectra were obtained at the Ohio State University Chemical Instrumentation Center.

Supporting Information Available: Synthesis and characterization of **1**, **3**, and **4**, and tables of rate constants (Tables S-1 through S-3) for the decomposition of **1**, formation of **3–6** during the decomposition of **1**, and the hydrolysis of authentic **3** and **4**. This material is available free of charge via the Internet at <http://pubs.acs.org>.

JO034505U

(12) Rangappa, K. S.; Novak, M. *J. Org. Chem.* **1992**, *57*, 1285–1290. Novak, M.; Rangappa, K. S.; Manitsas, R. K. *J. Org. Chem.* **1993**, *58*, 7813–7821.

(13) Williams, K. B.; Richard, J. P. *J. Phys. Org. Chem.* **1998**, *11*, 701–706.

(14) Hibino, S.; Sugino, E.; Kuwada, T.; Ogura, N.; Shintani, Y.; Satoh, K. *Chem. Pharm. Bull.* **1991**, *39*, 79–80. Kazerani, S.; Novak, M. *J. Org. Chem.* **1998**, *63*, 895–897.

(15) Novak, M.; Brodeur, B. A. *J. Org. Chem.* **1984**, *49*, 1142–1144.